

RESEARCH ARTICLE

View Article Online

View Journal | View Issue

Cite this: *Org. Chem. Front.*, 2023, **10**, 5579

Why is phenyl azide so unreactive in [3 + 2] cycloaddition reactions? Demystifying Sustmann's paradigmatic parabola†

Luis R. Domingo, *^a Mar Ríos-Gutiérrez ^a and Patricia Pérez *^b

The [3 + 2] cycloaddition (32CA) reactions of phenyl azide with a series of 25 ethylenes of different electronic activation have been studied within Molecular Electron Density Theory (MEDT) at the ω B97X-D/6-311G(d,p) computational level to understand the low reactivity of azides participating in 32CA reactions. Analysis of the reactivity indices allows characterizing phenyl azide as a moderate electrophile and a moderate nucleophile. The relative reaction rate constants k_r of twelve selected 32CA reactions, together with the electrophilicity ω and nucleophilicity N indices of the corresponding ethylenes, allow us to classify these 32CA reactions into four groups: (i) group A, involving supernucleophilic ethylenes and displaying a $k_r > 10^4$; (ii) group B, involving strained cyclic ethylenes and displaying a $k_r < 10^2$; (iii) group C, involving strongly electrophilic ethylenes and displaying a $k_r \leq 10^2$, and (iv) group D, involving moderately electrophilic and nucleophilic ethylenes and displaying a $k_r < 2$. These four groups are characterized in Sustmann's "parabolic correlation", which results from an inaccurate interpretation of the reactivity of phenyl azide, which is not an "ambiphilic species" but rather a moderate electrophile that reacts efficiently only with supernucleophilic ethylenes in reverse electron density flux (REDF) zw-type 32CA reactions.

Received 31st May 2023,
Accepted 22nd September 2023

DOI: 10.1039/d3qo00811h

rsc.li/frontiers-organic

1. Introduction

[3 + 2] cycloaddition (32CA) reactions are some of the most efficient synthetic methods for constructing five-membered heterocyclic compounds due to their ability to build organic cyclic motifs regio- and/or stereoselectively.^{1–4}

The knowledge of 32CA reactions is challenging for organic chemists due to the variable electronic structures of the three-atom-components (TACs) participating in these reactions.⁵ In the 1960s, Huisgen⁶ and Firestone⁷ independently proposed two different mechanisms: one involving 1,2-dipolar species and another one involving diradical intermediates, respectively.

Recent Molecular Electron Density Theory⁸ (MEDT) studies of 32CA reactions of the simplest TACs towards ethylene **5** have established a relationship between their electronic structure and reactivity.⁵ Accordingly, depending on the electronic structure of TACs, i.e., *pseudodiradical*, *pseudo(mono)radical*, carbene, or zwitterionic, 32CA reactions have been classified into

the corresponding reaction types (see Scheme 1);⁵ thus, while the *pdr-type* 32CA reaction of azomethine ylide **1** with ethylene **5** takes place very quickly,⁹ the *zw-type* 32CA reaction of nitrene **3** needs suitable nucleophilic/electrophilic activations to take place.¹⁰

Frontier molecular orbital (FMO) theory¹¹ has been widely used to understand reactivity and regioselectivity based on HOMO and LUMO analysis of isolated reactants. However, molecular orbitals (MOs), created in the 30s of the last century,¹² are only mathematical artifacts without any physical

Azomethine ylide 1	Azomethine imine 2	Nitrene 3	Nitrile ylide 4
Structure			
<i>pseudodiradical</i>	<i>pseudoradical</i>	zwitterionic	carbenoid
Reactivity			
<i>pdr-type</i>	<i>pmr-type</i>	<i>zw-type</i>	<i>cb-type</i>
1.0 kcal/mol	7.7 kcal/mol	13.4 kcal/mol	7.8 kcal/mol

Scheme 1 Electronic structures of the simplest TACs and proposed reactivity types in 32CA reactions. MPWB1K/6-311G(d) gas phase activation energies of the non-polar 32CA reactions between the four simplest TACs **1–4** and ethylene **5** are given in kcal mol^{–1}.

^aDepartment of Organic Chemistry, University of Valencia, Dr Moliner 50, 46100 Burjassot, Valencia, Spain. E-mail: luisrdomingo@gmail.com

^bUniversidad Andrés Bello, Facultad de Ciencias Exactas, Departamento de Ciencias Químicas, Centre for Theoretical and Computational Chemistry, Av. República 275 8370146, Chile. E-mail: p.perez@unab.cl

† Electronic supplementary information (ESI) available. See DOI: <https://doi.org/10.1039/d3qo00811h>



reality used only for the construction of the molecular wave function, which provides the distribution of the electron density, which is the only observable.¹³

In 1972, Sustmann and Trill analyzed the HOMO and LUMO energy gaps between phenyl azide **6**, Ph-N₃, and a series of substituted ethylenes to understand the reactivity of this TAC in 32CA reactions.¹⁴ They proposed that in these 32CA reactions of phenyl azide **6**, the reactivity is increased by both electron-releasing (ER) and electron-withdrawing (EW) substituents in the ethylene, in a reaction classified as “inverse electron demand”.¹⁴ Since the LUMO energies were unknown, and the HOMO and LUMO energies should be shifted in the same direction by any substituent, Sustmann and Trill used the HOMO energies of the ethylenes as a measure of the decrease in LUMO energies. When the logarithms of the second order rate constant *k* were represented *versus* the ionization potentials (IPs) of the substituted ethylenes, as a measure of the HOMO energies, a parabola graph was obtained for the first time (see Fig. 1).¹⁴ However, as this parabola shows, only three vinyl amines and two strained cyclic ethylenes are activated in these 32CA reactions.

At the same time, Sustmann and Schubert studied the substituent effects on the diene in Diels–Alder (DA) reactions. For this purpose, the second order rate constants of DA reactions of tetracyanoethylene **7**, one of the most electrophilic ethylenes, with a series of substituted dienes were analyzed.¹⁵ When the logarithms of the rate constants *k* of these DA reac-

tions were represented *versus* the $E_{\text{HOMO}} - E_{\text{LUMO}}$ gaps, a good hyperbola, instead of a parabola as in Fig. 1, was obtained.¹⁵ Note that in this case, Sustmann studied the polar DA reactions of strongly electrophilic tetracyanoethylene **7** with a series of dienes of increased nucleophilicity, while in the former study, he used both nucleophilic and electrophilic ethylene and acetylene derivatives with phenyl azide **6**.

Very recently, Liu *et al.* reported a computational exploration of azides’s “ambiphilic reactivity” based on Sustmann’s paradigmatic parabola.¹⁶ They suggested that both distortion/interaction energy¹⁷ and activation strain models¹⁸ justify Sustmann’s IPs of ethylenes as a powerful predictor of reactivity. These authors added to Sustmann’s ethylene series two strained cycloethylenes and cyclooctyne **8** used in bioorthogonal chemistry, showing how these fit into the MO energy criteria often used to understand cycloaddition reactivity.

Recently, the strain-promoted 32CA (SP-32CA) reactions of phenyl azide **6** with a series of cycloalkynes, including cyclooctyne **8**, were studied within MEDT.¹⁹ That study revealed an excellent linear correlation between the reduction in activation enthalpy and the decrease in the ring size of these cycloalkynes, as a result of the reduction in ring strain. That study established that the loss of the ring strain along the reaction path and the easy depopulation of the C–C≡C–C bonding region of the strained cycloalkynes along the reaction are responsible for the kinetics and thermodynamics of these SP-32CA reactions, rather than the previously suggested concept of “less distortion of the 1,3-dipole in the transition state geometry”.²⁰ These SP-32CA reactions showed a low global electron density transfer²¹ (GEDT) at the corresponding transition state structures (TS), indicating the low polar character of these reactions, which were classified as null electron density flux (NEDF).^{22,23}

The classical azide–alkyne 32CA reactions described by Huisgen²⁴ require elevated temperatures to achieve reasonable reaction rates. Indeed, the simplest azide **9**, HN₃, is a zwitterionic TAC presenting a high activation energy towards ethylene **5**, 19.5 kcal mol^{−1}.¹⁷ Thus, it is expected that, just as in other *zw-type* 32CA reactions, the electrophilic/nucleophilic activation of both azide **9** and ethylene **5** decreases this unfavorable activation energy.

However, a recent experimental and MEDT study of the thermal 32CA reactions of aryl azides **10** with acetylenes **11** showed that substituting both the azide and the acetylene only slightly modifies the unfavorable reaction conditions demanded in these *zw-type* 32CA reactions, with no significant improvement.²⁵ In addition, a mixture of the two regioisomeric 1,2,3-triazoles **12** and **13** was obtained in all cases (see Scheme 2).²⁵

Nitrones are nucleophilic zwitterionic TACs participating in *zw-type* 32CA reactions. However, their reactivity is more susceptible to substitution than that of azides. In 2018, the *zw-type* 32CA reactions of *C,N*-dimethyl nitron **14** with a series of ethylenes of increased electrophilic character were studied within MEDT as a model of 32CA reactions of experimental cyclic nitrones (see Scheme 3).¹⁰ The activation energies of

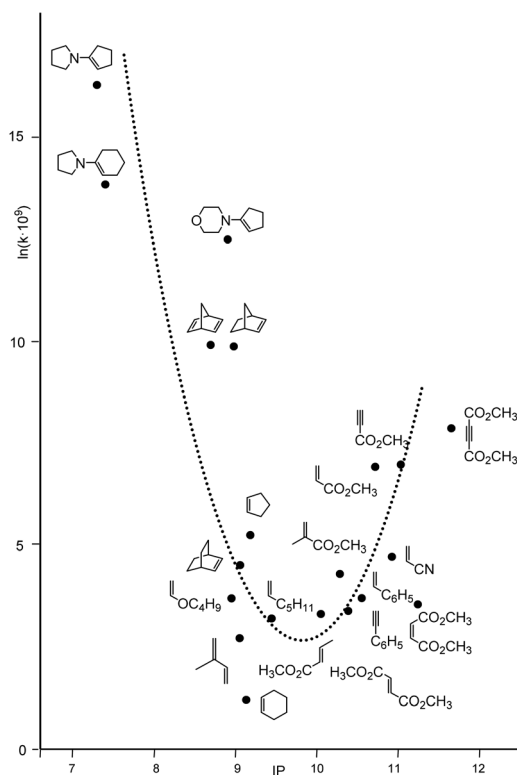
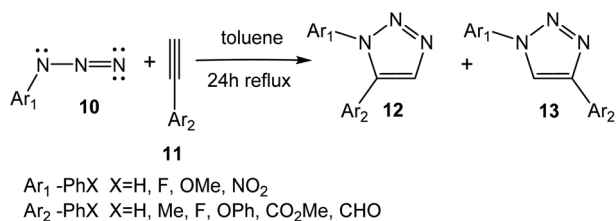
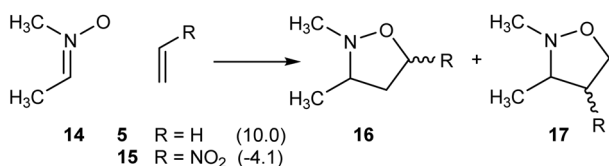


Fig. 1 Sustmann’s parabolic correlation of the logarithms of the second order rate constants *k* vs. the IPs, in eV, of substituted ethylenes.





Scheme 2 32CA reactions of substituted aryl azides **10** with aryl substituted acetylenes **11**.



Scheme 3 Zw-type 32CA reactions of C,N-dimethyl nitron **14** with ethylene **5** and nitroethylene **15**. Relative energies of the TSs, with respect to the separated reagents, are given in parenthesis in kcal mol⁻¹.

these *zw-type* 32CA reactions decreased up to 14.1 kcal mol⁻¹ when using strongly electrophilic ethylenes such as nitroethylene **15**.¹⁰ In addition, these polar reactions were found to be completely *meta* regioselective, yielding the *meta* isoxazolidines **17** exclusively, unlike the reactions of azides with electrophiles, which show poor regioselectivity (see Scheme 3).²⁵

Herein, an MEDT study of the *zw-type* 32CA reactions of phenyl azide **6** with a series of 25 ethylenes of different electrophilic/nucleophilic activation is reported to understand the low reactivity of azides compared with other zwitterionic TACs such as nitrones (see Chart 1). Additionally, a chemical rationalization of Sustmann's parabolic correlation is pro-

vided. The reason for the low reactivity of substituted aryl azides is discussed in section 4 in the ESI† (see Scheme 2).

2. Results and discussion

2.1. Analysis of the electronic structure and chemical properties at the GS of the reagents

2.1.1. Analysis of the electronic structure of the reagents.

Before studying the 32CA reactions of phenyl azide **6** with the selected ethylenes, the electronic structures of the simplest azide **9**, phenyl azide **6**, and two substituted phenyl azides, **42** and **43**, were investigated through a topological analysis of the Electron Localization Function²⁶ (ELF). The ELF permits quantitative characterization of the electron density distribution in a molecule,²⁷ allowing the classification of TACs into one of the four types found within MEDT, and thus establishing a correlation between their electronic structure and their reactivity in 32CA reactions (see Scheme 1). The complete ELF analysis of the four azides and three selected ethylenes is given in section 1 in the ESI.† Herein, only the ELF analysis of phenyl azide **6** is discussed (Fig. 2).

ELF topological analysis of phenyl azide **6** reveals the presence of two V(N1,N2) and V'(N1,N2) disynaptic basins, integrating a total of 4.13 e, one V(N2,N3) disynaptic basin integrating 2.49 e, and two V(N1) and V(N3) monosynaptic basins, integrating 3.78 and 3.38 e, respectively. While the population of the two V(N1,N2) and V'(N1,N2) disynaptic basins allows relating the N1–N2 bonding region to a double bond, that of the V(N2,N3) disynaptic basin allows associating the N2–N3 bonding region with a populated single bond within Lewis's bonding model. The V(N1) and V(N3) monosynaptic basins are associated with non-bonding electron density regions at the N1 and N3 nitrogens. Thus, the absence of any *pseudoradical* center or a carbenoid carbon at this species allows classifying phenyl azide **6** as a zwitterionic TAC participating in *zw-type* 32CA reactions. The ELF topology of the four azides given in the ESI† indicates that substituting the hydrogen of the sim-

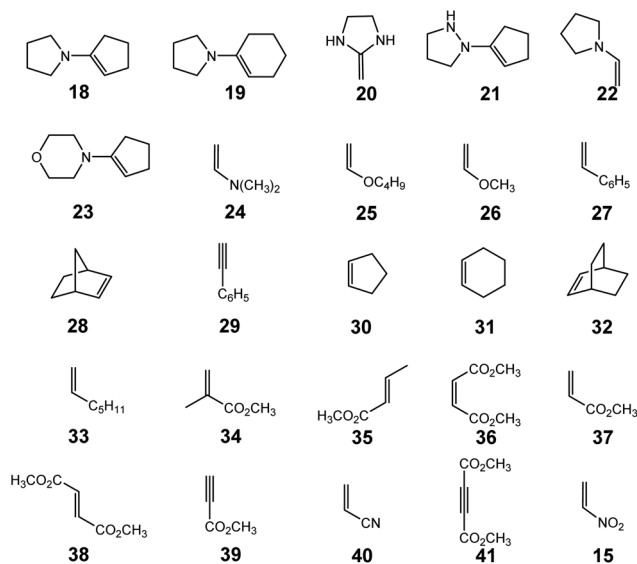


Chart 1 Structures of 25 ethylenes selected in this MEDT study.

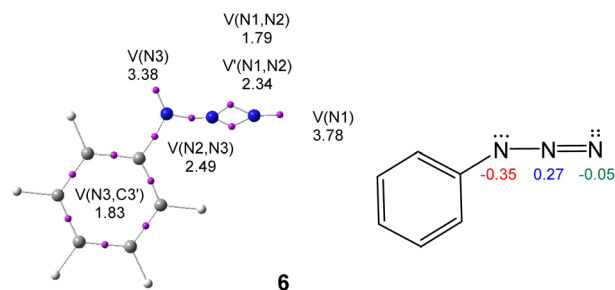


Fig. 2 ELF basin attractor positions, together with the most relevant valence basin populations and ELF-based Lewis-like structure together with natural atomic charges of phenyl azide **6**, computed at the ωB97X-D/6-311G(d,p) level in the gas phase. Valence basin populations and natural atomic charges are given as the average number of electrons, e. Negative charges are colored in red, positive in blue, and negligible in green.



plest azide **9** with aryl substituents does not significantly modify the GS electronic structure of these zwitterionic TACs.

The complete ELF topological analysis of the nucleophilic vinyl amine **22**, strained cyclopentene **30**, and electrophilic acrylonitrile **40** is given in section 1 of the ESI.† The ELF analysis shows that substitution on the C–C double bond does not significantly modify the electronic structure of these alkenes. All ethylenes are characterized by the presence of two V(C4,C5) and V(C4,C5) disynaptic basins integrating a total population ranging from 3.56 e (vinyl amine **22**) to 3.35 e (acrylonitrile **40**).

The natural atomic charges^{28,29} of phenyl azide **6** indicate that while the two N1 and N3 nitrogens of phenyl azide **6** are negatively charged by -0.05 and -0.35 e, respectively, the central N2 nitrogen is positively charged by $+0.27$ (see Fig. 2). This charge distribution, which differs from the one typically associated with the traditional 1,2-dipolar structure of azides, is a consequence of the total electron density distribution in the N–N–N core of this TAC, which is only determined by the presence of the three nitrogen nuclei and not by any resonance analysis.⁵ Note that the N–N–N core of this TAC is negatively charged by -0.13 e.

2.1.2 Analysis of the chemical properties of the reagents.

Next, the chemical reactivity of azides and the 25 ethylenes was studied by analyzing the reactivity indices^{30,31} at the GS of the reagents. The analysis of quantum chemical reactivity indices has proven to be a powerful tool for understanding reactivity in polar cycloaddition reactions.^{31,32} The reactivity indices were calculated at the B3LYP/6-31G(d) computational level since it was used to establish the electrophilicity and nucleophilicity scales.³¹ The analysis of global reactivity indices, namely, the electronic chemical potential μ , chemical hardness η , electrophilicity ω , and nucleophilicity N , for the azides and the substituted ethylenes is given in section 2 of the ESI.† Herein, those of phenyl azide **6** and the ethylenes are briefly commented on.

Phenyl azide **6** presents an electrophilicity ω index³³ of 1.27 eV and a nucleophilicity N index³⁴ of 2.92 eV, being classified as a moderate electrophile and a moderate nucleophile (see Table S1 in section 2 of the ESI†). Consequently, the analysis of the reactivity indices of phenyl azide **6** does not characterize it as an ambiphilic species,^{35,36} as was suggested,¹⁶ as it is neither a strongly electrophilic nor a strongly nucleophilic species participating in polar reactions. Note that polar reactions demand the participation of strongly electrophilic and nucleophilic reagents. A thorough discussion of the concept of ambiphilic species is presented in section 3 of the ESI.†

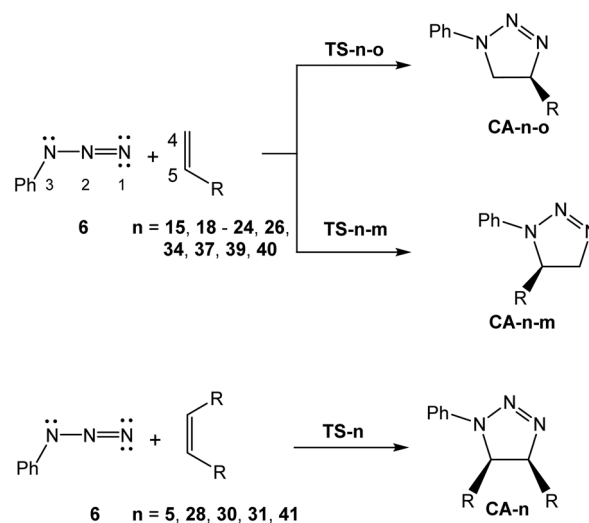
Table S2 in section 2 of the ESI† shows the reactivity indices of the 25 ethylenes selected for this MEDT study (see Chart 1) in descending order of their nucleophilicity N index. Ethylenes **18–28** have nucleophilicity N indices higher than 3.0 eV, thus being classified as strong nucleophiles participating in polar reactions. Of noteworthy significance, vinyl amines **18** to **23** display exceptionally elevated nucleophilicity N indices, surpassing 4.0 eV, which categorizes them as supernucleophiles able to react even with moderate electrophiles in a polar

reaction.³² Compounds **29–33** have nucleophilicity N indices between 2.00 and 2.84 eV, being classified as moderate nucleophiles. Some of them are strained cyclic ethylenes. Finally, ethylenes **15**, **36–41** have electrophilicity ω indices higher than 1.50 eV, being classified as strongly electrophilic species.

The electronic chemical potentials³⁷ μ of the supernucleophilic vinyl amines **18–23**, between -1.42 and -1.87 eV, are higher than that of phenyl azide **6**, $\mu = -3.62$ eV. Consequently, along the corresponding polar 32CA reactions, the flux of the electron density will take place from ethylenes **18–23** towards phenyl azide **6**, and these 32CA reactions are classified as reverse electron density flux (REDF).^{23,38} On the other hand, strongly electrophilic ethylenes **15**, **36–41** have electronic chemical potentials μ lower than -4.11 eV; consequently, it is expected that along a polar reaction, the flux of the electron density will take place from phenyl azide **6** towards these electrophilically activated ethylenes. In this scenario, these 32CA reactions are classified as forward electron density flux (FEDF).^{23,38} Note that Sustmann classified all these 32CA reactions indistinctly as “type II, in which the HOMO and LUMO energies of the reagents should be considered”.¹⁴

2.2. Study of the *zw*-type 32CA reactions of phenyl azide **6** with 18 ethylenes of different electronic activation

In order to gain insights into the participation of azide **6** in *zw*-type 32CA reactions, the reactions with 18 ethylenes presenting different electronic activation were studied. They include strongly nucleophilically activated vinyl amines and vinyl ethers such as **18–24** and **26**, strained cycloalkenes such as **28** and **30**, electrophilic ethylenes such as **15**, **34**, **37**, and **39–41**, and the low reactive ethylene **5**. Most are monosubstituted ethylenes; consequently, two regioisomeric reaction paths, *ortho* and *meta*, are feasible along the corresponding *zw*-type 32CA reactions (see Scheme 4). Analysis of the stationary points involved in these 32CA reactions reveals that they



Scheme 4 Reaction paths associated with the 32CA reactions of phenyl azide **6** with the selected 18 ethylenes.



take place *via* a one-step mechanism. The relative electronic energies of all stationary points are given in Table 1, while the total electronic energies are gathered in Table S10 in the ESI.†

For a comparative analysis, the activation energy of the 32CA reaction of phenyl azide **6** with ethylene **5**, 17.9 kcal mol⁻¹, is taken as the reference of the unfavorable non-polar *zw*-type 32CA reactions of this azide (see Table S11 in the ESI†). Some appealing conclusions can be obtained from the analysis of the relative energies given in Table 1: (i) the activation energies of the 32CA reactions shown in Scheme 4 range from 18.6 (TS-31) to 6.3 (TS-21-*m*) kcal mol⁻¹. While the 32CA reaction with acrylonitrile **40**, a strong electrophile ($\omega = 1.74$ eV), presents an activation energy, 17.2 kcal mol⁻¹, similar to that with ethylene **5**, the activation energy of the 32CA reaction involving vinyl amine **21**, a supernucleophile ($N = 4.40$ eV), experiences a considerable lowering of 11.5 kcal mol⁻¹; (ii) while the activation energy of the 32CA reaction involving the most electrophilic nitroethylene **15** ($\omega = 2.61$ eV), not included in the Sustmann's series, decreases by only 3.4 kcal mol⁻¹, the activation energies of those involving the supernucleophilic ethylenes **18–23** ($N > 4.00$ eV) are lowered by 9.9 kcal mol⁻¹ on average. These behaviors indicate a clear preferential reactivity of phenyl azide **6** towards supernucleophilic ethylenes; (iii) the activation energies of 32CA reactions involving strained cycloalkenes **28** and **30** are lowered by 4.9 and

2.8 kcal mol⁻¹ with respect to that involving ethylene **5**; (iv) the regioselectivity in these 32CA reactions ranges from 1.0 (TS-15-*o*) to 17.6 (TS-20-*m*) kcal mol⁻¹; (v) the 32CA reactions of phenyl azide **6** with electrophilic ethylenes are poorly *ortho* regioselective, while those involving strongly nucleophilic ethylenes are completely *meta* regioselective; (vi) all 32CA reactions are exothermic by at least 24.9 kcal mol⁻¹ (CA-40-*o* and CA-40-*m*). Consequently, these 32CA reactions are irreversible and, therefore, kinetically controlled; finally, (vii) considering the activation energies and the regioselectivities given in Table 1, only the *zw*-type 32CA reactions of phenyl azide **6** with supernucleophilic vinyl amines **18–23** can be regarded as kinetically activated (see later).

A graphical representation of the activation energies of the eighteen 32CA reactions *versus* the nucleophilicity N indices of the substituted ethylenes given in Table S2 in section 2 of the ESI† shows an acceptable polynomial correlation; $R^2 = 0.80$ (see Fig. 3a). The activation energies of 32CA reactions depend on several contributing factors, such as the electronic structure of the TAC, the nucleophilic/electrophilic interactions at the TSs, the use of strained reagents, and so forth. Among them, the polar nature of the reaction, quantified using the GEDT at the TSs,²¹ plays a particularly relevant role in the activation barriers of *zw*-type 32CA reactions as it is the most significant factor decreasing the unfavorable activation energies associated with these *zw*-type 32CA reactions.⁵ Fig. 3b shows that when only nucleophilic ethylenes are considered, *i.e.*, ethylenes with $N \geq 3.0$ eV, a linear correlation is obtained with an $R^2 = 0.83$. Analysis of the polynomial curve shown in Fig. 3a, similar to that reported by Sustmann,¹⁴ shows that rather than a parabolic relationship, the activation energy mainly depends on the nucleophilic character of the ethylene. It is noteworthy that reactions involving strong electrophiles such as **15** and **41** present activation energies higher than 14.4 kcal mol⁻¹ (see Table 1).

Liu *et al.* included a series of three strained unsaturated cyclic compounds to the Sustmann's ethylene series given in Fig. 1.¹⁶ Cyclooctyne **8** experienced the largest acceleration, $\Delta E = 9.9$ kcal mol⁻¹, despite the low nucleophilic character of this cycloalkyne, $N = 2.38$ eV,¹⁹ which characterizes **8** as a moderate nucleophile. When cyclooctyne **8** is included in Fig. 3a, a substantial deviation is observed. A similar behavior was found by Liu *et al.*¹⁶ This behavior is easily explained by the fact that the significant acceleration of the corresponding SP-32CA reaction is not attributable to the polar nature of the reaction, GEDT = -0.03 e, but rather to the loss of the ring strain along the reaction pathway.¹⁹ This behavior was reinforced by the strong exothermic character of the corresponding SP-32CA reaction, $\Delta E = -81.9$ kcal mol⁻¹. Note that the non-polar 32CA reaction of methyl propiolate **39**, a linear alkyne, has an activation energy of 16.1 kcal mol⁻¹, being exothermic by -74.5 kcal mol⁻¹.¹⁹

The C–N distances of the two pairs of interacting nitrogen and carbon centers at the *ortho* and *meta* TSs associated with the eighteen 32CA reactions are given in Table 2, together with the geometric asynchronicity, Δl , while the structures of the *ortho* and *meta* TSs of two representative 32CA reactions are

Table 1 ω B97X-D/6-311G(d,p) gas phase relative electronic energies, ΔE in kcal mol⁻¹, of the stationary points involved in the 32CA reactions of phenyl azide **6** with the selected 18 ethylenes

	ΔE	$\Delta\Delta E(m-o)$		ΔE
TS-18- <i>o</i>	17.5		CA-18- <i>o</i>	-32.9
TS-18- <i>m</i>	6.4	-11.1	CA-18- <i>m</i>	-30.4
TS-19- <i>o</i>	20.5		CA-19- <i>o</i>	-29.8
TS-19- <i>m</i>	8.6	-11.9	CA-19- <i>m</i>	-27.4
TS-20- <i>o</i>	27.2		CA-20- <i>o</i>	-26.5
TS-20- <i>m</i>	9.7	-17.6	CA-20- <i>m</i>	-25.0
TS-21- <i>o</i>	15.9		CA-21- <i>o</i>	-37.8
TS-21- <i>m</i>	6.3	-9.5	CA-21- <i>m</i>	-32.6
TS-22- <i>o</i>	20.3		CA-22- <i>o</i>	-27.3
TS-22- <i>m</i>	10.0	-10.3	CA-22- <i>m</i>	-28.2
TS-23- <i>o</i>	17.1		CA-23- <i>o</i>	-33.8
TS-23- <i>m</i>	6.9	-10.3	CA-23- <i>m</i>	-30.9
TS-24- <i>o</i>	21.0		CA-24- <i>o</i>	-28.3
TS-24- <i>m</i>	11.5	-9.5	CA-24- <i>m</i>	-29.0
TS-26- <i>o</i>	20.1		CA-26- <i>o</i>	-31.3
TS-26- <i>m</i>	14.9	-5.2	CA-26- <i>m</i>	-31.6
TS-28	12.9		CA-28	-42.6
TS-30	15.1		CA-30	-35.8
TS-31	18.6		CA-31	-30.5
TS-34- <i>o</i>	16.9		CA-34- <i>o</i>	-28.3
TS-34- <i>m</i>	14.7	-2.2	CA-34- <i>m</i>	-27.0
TS-37- <i>o</i>	15.8		CA-37- <i>o</i>	-27.7
TS-37- <i>m</i>	13.6	-2.2	CA-37- <i>m</i>	-28.8
TS-39- <i>o</i>	17.4		CA-39- <i>o</i>	-77.5
TS-39- <i>m</i>	16.1	1.3	CA-39- <i>m</i>	-74.5
TS-40- <i>o</i>	17.2		CA-40- <i>o</i>	-24.9
TS-40- <i>m</i>	18.2	1.0	CA-40- <i>m</i>	-24.9
TS-41	15.5		CA-41	-75.0
TS-15- <i>o</i>	14.5		CA-15- <i>o</i>	-29.1
TS-15- <i>m</i>	15.4	1.0	CA-15- <i>m</i>	-31.8
TS-5	17.9		CA-0	-31.7



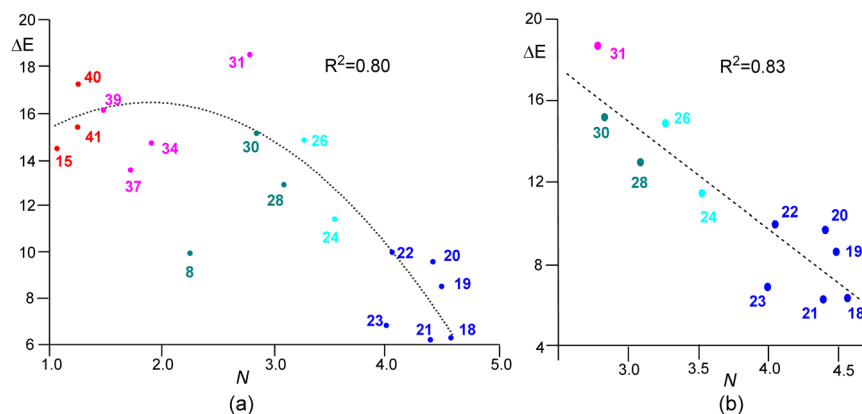


Fig. 3 Plot of the activation energy, ΔE in kcal mol⁻¹, versus the nucleophilicity N index, in eV, for (a) the 18 selected ethylenes and (b) only nucleophilic ethylenes. Supernucleophilic ethylenes are given in dark blue, strongly nucleophilic ethylenes are given in light blue, marginally electrophilic and nucleophilic ethylenes are given in pink and strongly electrophilic ethylenes are given in red. Strained cyclic ethylenes are given in green. The data for the 32CA reaction involving strained cyclooctyne **8** are included.

Table 2 C–N distances Å of the two pairs of interacting centers at the *ortho* and *meta* TSs associated with the eighteen 32CA reactions. The GEDT values computed at the TSs are given as the average number of electrons, e

	<i>ortho</i>		Δl	GEDT	<i>meta</i>		Δl	GEDT
	l(N1–C5)	l(N3–C4)			l(N1–C4)	l(N3–C5)		
18	2.227	2.142	0.09	−0.19	2.023	2.656	0.63	−0.36
19	2.191	2.134	0.06	−0.24	1.992	2.603	0.61	−0.42
20	2.281	2.065	0.22	−0.24	1.969	2.783	0.81	−0.42
21	2.240	2.147	0.09	−0.17	2.005	2.607	0.60	−0.34
22	2.216	2.076	0.14	−0.19	1.992	2.536	0.54	−0.34
23	2.234	2.133	0.10	−0.19	2.026	2.637	0.61	−0.35
24	2.216	2.082	0.13	−0.17	1.974	2.507	0.53	−0.33
26	2.155	2.113	0.04	−0.12	1.976	2.341	0.37	−0.25
34	2.215	2.049	0.17	0.00	1.998	2.225	0.23	−0.03
37	2.214	2.030	0.18	0.02	1.995	2.195	0.20	−0.01
39	2.232	2.056	0.17	0.05	2.063	2.180	0.12	0.02
40	2.232	2.002	0.23	0.04	1.999	2.181	0.18	0.01
15	2.242	1.985	0.26	0.09	2.000	2.166	0.17	0.04
28	2.163	2.220	0.06	−0.07				
30	2.109	2.208	0.10	−0.10				
31	2.070	2.195	0.13	−0.12				
41	2.147	2.714	0.57	0.07				
5	2.123	2.132	0.01	−0.07				

shown in Fig. 4. Some appealing conclusions can be obtained from the geometric parameters given in Table 2: (i) all N–C distances, which are longer than 1.80 Å, indicate that the N–C single bond formation has not started yet in any TS;⁵ (ii) all TSs correspond to asynchronous N–C single bond formation processes; (iii) the asynchronicity ranges from $\Delta l = 0.06$ Å at **TS-28**, involving symmetric strained cyclic ethylene **28**, to $\Delta l = 0.81$ Å at **TS-20-*m***, involving vinyl amine **20**; (iv) the more favorable *meta* TSs involving supernucleophilic vinyl amines **18–23** are more asynchronous than the *ortho* ones, while *ortho* TSs involving electrophilic ethylenes **15** and **40** are more asynchronous than the *meta* ones. This behavior is a consequence of the fact that the N1 nitrogen is the most electrophilic center of phenyl azide **6**, while the N3 nitrogen is the most nucleophilic one (see the electrophilic and nucleophilic Parr functions of azides **9** and **44** in Fig. S3 in section 2 of the ESI†).

Analysis of the GEDT at the TSs involved in these *zw-type* 32CA reactions allows for the quantification of the polar character of these cycloaddition reactions.²¹ Table 2 shows the GEDT values computed at all TSs. GEDT values lower than 0.05 e correspond to non-polar processes, while values higher than 0.20 e correspond to highly polar processes. On the other hand, the sign of the GEDT computed at the TACs unambiguously allows the classification of the polar 32CA reactions as FEDF, with $\text{GEDT} > +0.05$ e , and REDF, with $\text{GEDT} < -0.05$ e .^{23,38} The sign of the GEDT values indicates that phenyl azide **6** is positively or negatively charged at the corresponding TSs. Non-polar 32CA reactions characterized by a negligible $\text{GEDT} \leq |0.05|$ e are classified as NEDF.^{22,23} Note that the sign of the GEDT in NEDF reactions has no chemical meaning. A comparative analysis of the GEDT values obtained by using the ω B97X-D and M06-



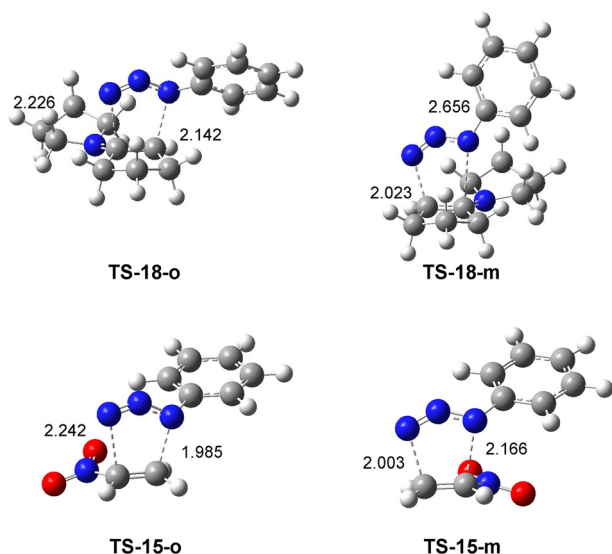


Fig. 4 ω B97X-D/6-311G (d,p) gas phase optimized geometries of the *ortho* and *meta* regioisomeric TSs involved in the 32CA reactions of phenyl azide **6** with supernucleophilic vinyl amine **18** and strongly electrophilic nitroethylene **15**. Distances are given in angstroms, Å.

2X functionals shows that both accurately describe the same polar character (see section S5 in the ESI†).

The GEDT values at the more favorable regioisomeric TSs computed at the phenyl azide framework range from -0.42 e at **TS-19-m** to 0.09 e at **TS-15-o**. In particular, the *meta* TSs associated with the more favorable *zw-type* 32CA reactions involving supernucleophilic vinyl amines **18–23** exhibit a notably high polar character, $\text{GEDT} > -0.34$ e, and the reactions are classified as REDF. Conversely, the *ortho* TSs involving strongly electrophilic ethylenes such as nitroethylene **15** present a very low polar character, $\text{GEDT} < 0.09$ e, and the reactions are classified as FEDF. Many 32CA reactions of phenyl azide **6** present $\text{GEDT} \leq |0.05|$ e, indicating the non-polar character of these 32CA reactions, classified as NEDF. This fact accounts for the high activation energy of these *zw-type* 32CA reactions.⁵ Note that these results can be anticipated by the analysis of the electronic chemical potential of the reagents (see section 2.1).

A graphical representation of the GEDT values computed at the more favorable regioisomeric TSs of the eighteen 32CA reactions *versus* the nucleophilicity N index of the substituted ethylenes shows a very good linear correlation; $R^2 = 0.94$ (see Fig. 5). As the feasibility of a *zw-type* 32CA reaction mainly depends on the polar character of the reaction, this figure indicates that the ethylene should have an $N > 3.5$ eV to favor a GEDT higher than 0.30 e. Many reactions involving substituted ethylenes with $N < 3.0$ eV present GEDT values lower than 0.10 e, and the reaction is low-polar or non-polar as the GEDT is $\leq |0.05|$. Consequently, these *zw-type* 32CA reactions are very unfavorable.

Liu *et al.* obtained similar GEDT values for the 32CA reactions of phenyl azide **6**, although they did not discuss either the polar reactivity or the electron density flux along these

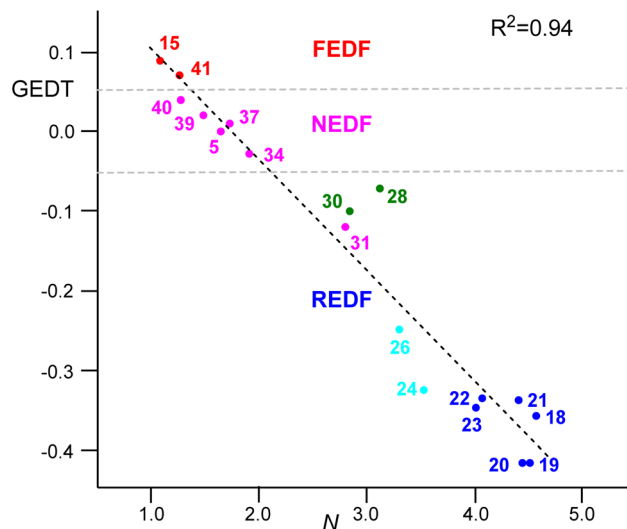


Fig. 5 Plot of the GEDT values computed at the more favorable TSs, in e, *versus* the nucleophilicity N index, in eV. Supernucleophilic ethylenes are given in dark blue, strongly nucleophilic ethylenes in light blue, marginally electrophilic and nucleophilic ethylenes in pink, strongly electrophilic ethylenes in red, and strained cyclic ethylenes in green.

32CA reactions.¹⁶ Interestingly, many of these 32CA reactions with electrophilic ethylenes presented a $\text{GEDT} \leq |0.03|$ e,¹⁶ showing the non-polar character of these cycloaddition reactions and, consequently, the non-ambiphilic character of phenyl azide **6**. This behavior is a consequence of the moderate nucleophilic character of this zwitterionic TAC.

In 2002, the first theoretical electrophilicity scale based on Parr's electrophilicity ω index³³ for a series of dienes and ethylenes participating in Diels–Alder reactions was established.³⁹ In the absence of a nucleophilicity index, a relationship between the inverse of Parr's electrophilicity ω index and the nucleophilicity of the studied species, and *vice versa*, was established within this series of dienes and ethylenes.³⁹ Thus, ethylenes with $N < 1.7$ eV, which are considered marginal nucleophiles, correspond to strong electrophiles (see Table S2 in section 2 of the ESI†). As depicted in Fig. 5, a reversal in the electron density flux is observed for ethylenes possessing N values < 1.7 eV, signifying their classification as strong electrophiles. Unfortunately, this inversion is not sufficient to activate these *zw-type* 32CA reactions. Note that although it causes an inversion in Sustmann's parabola, it has no chemical significance regarding the activation of these highly unfavorable *zw-type* reactions of azides.

Depending on the nucleophilic/electrophilic behaviors of the ethylenes, these *zw-type* 32CA reactions can be classified as (i) FEDF, involving electrophilic ethylenes with $\omega > 1.70$ eV; (ii) NEDF, for non-polar 32CA reactions involving moderately nucleophilic/electrophilic ethylenes; and (iii) REDF, involving strained cyclic ethylenes and strongly nucleophilic ethylenes with $N > 3.00$ eV (see Fig. 5). As the *zw-type* 32CA reactions are notably accelerated by an increase of the polar character of the reaction, this graph accounts for the fact that only supernu-



cleophilic species, with an $N > 4.00$ eV, accelerate these 32CA reactions effectively. Consequently, analysis of the nucleophilicity N index of ethylenes can predict the feasibility of these 32CA reactions of azides.

Using the Eyring–Polanyi equation,⁴⁰ the relative reaction rate constants k_r of the 32CA reaction of phenyl azide **6** with a series of 12 selected ethylenes, with respect to that of ethylene **5**, were computed (see Table 3). The corresponding thermodynamic parameters are given in Table S11 in the ESI.†

The relative reaction rate constants k_r range from 8.58×10^{-2} (**31**) to 2.62×10^5 (**21**). Analysis of the relative reaction rate constants k_r given in Table 3 permit us to classify the 32CA reactions of phenyl azide **6** studied by Sustmann into four groups of different chemical reactivity (see Fig. 6): (i) group A, involving supernucleophilic ethylenes, presenting a k_r between 2.62×10^5 and 3.50×10^4 ; (ii) group B, involving strained cyclic ethylenes, presenting a k_r between 65 and 1.7. Note that the three strained ethylenes of group B exhibit clear activation compared to cyclohexene **31**; (iii) group C, involving strongly electrophilic ethylenes with a $k_r \leq 1.00 \times 10^2$; and finally, (iv) group D, involving poorly activated electrophilic/nucleophilic ethylenes with a $k_r < 2.00$. These groups are identified in four non-overlapping zones on the hypothetical Sustmann's parabolic graph (see Fig. 6).

The 32CA reaction of cyclohexene **31**, a non-strained cyclic ethylene, is 0.1 times slower than that with ethylene **5**. As can be observed, only the 32CA reactions involving ethylenes of group A can be considered strongly activated electronically. Interestingly, although the strain in cyclic ethylenes can accelerate the 32CA reaction by 10^2 times, adequate nucleophilic activation of the ethylene can accelerate it by more than 10^4 times.

When the logarithms of the relative reaction rate constants k_r of the 32CA reactions of phenyl azide **6** with nucleophilic ethylenes with $N > 2.70$ eV are plotted *versus* the nucleophilicity N index, a linear correlation is obtained with an $R^2 = 0.90$ (see Fig. 7). This figure leads to two relevant conclusions: (i) the logarithm of the relative reaction rate constants k_r responds linearly only for strongly nucleophilic ethylenes, and

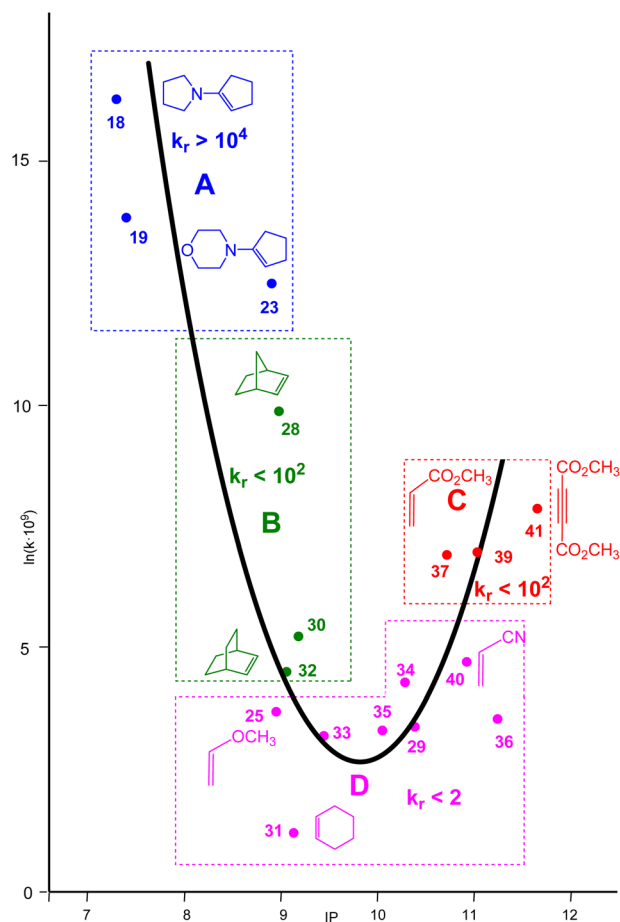


Fig. 6 Classification of Sustmann's ethylenes into (A) supernucleophilic ethylenes, in blue; (B) strained cyclic ethylenes, in green; (C) strongly electrophilic ethylenes, in red; and (D) weakly electrophilic/nucleophilic ethylenes, in pink.

Table 3 Activation Gibbs free energies, ΔG in kcal mol⁻¹, computed in toluene at 110 °C, and relative reaction rate constants, k_r , for 12 selected 32CA reactions involving phenyl azide **6**

Group		ΔG	k_r
	5	33.58	1.00
A	18	24.17	2.32×10^5
A	19	25.61	3.50×10^4
A	21	24.08	2.62×10^5
A	23	24.72	1.13×10^5
B	28	30.40	6.49×10^1
B	30	33.16	1.73
D	31	35.45	8.58×10^{-2}
D	37	33.02	2.09
D	39	33.09	1.90
D	40	33.96	6.08×10^{-1}
C	15	31.96	8.43
C	41	30.07	1.00×10^2

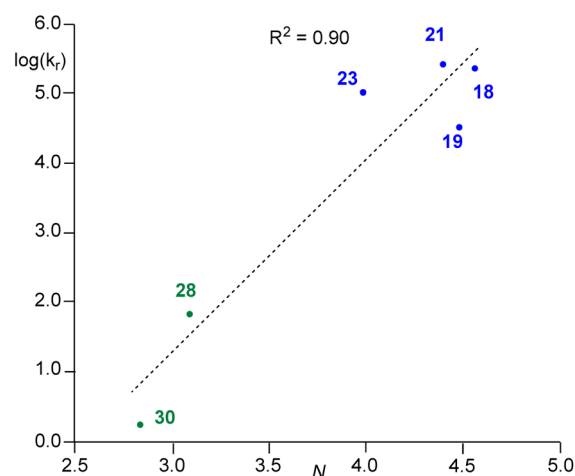


Fig. 7 Plot of the logarithm of the relative reaction rate constants k_r of the 32CA reactions of phenyl azide **6** with supernucleophilic and strongly nucleophilic ethylenes *versus* the nucleophilicity N index, in eV. Supernucleophilic ethylenes are highlighted in dark blue, while strained cyclic ethylenes are in green.



(ii) only supernucleophilic ethylenes with $N > 4.0$ eV effectively accelerate the *zw-type* 32CA reactions of phenyl azide **6**.

2.3. Characterization of the *zw-type* reactivity of phenyl azide **6**. Analysis of the formation of the two N–C single bonds along the 32CA reaction

To characterize the *zw-type* reactivity of aryl azides, a Bonding Evolution Theory⁴¹ (BET) analysis of the bonding changes along the more favorable *meta* regioisomeric reaction path associated with the 32CA reaction between phenyl azide **6** and vinyl amine **22** was performed. BET enables a detailed description of molecular mechanisms in terms of bonding changes characterized through variations of ELF electron populations along the reaction path. The complete BET analysis is reported in section 6 of the ESI.† ELF basin attractor positions, together with the most significant valence basin populations, of the structures of the intrinsic reaction coordinate (IRC) path involved in the formation of the two new N–C single bonds are shown in Fig. 8.

From the BET analysis the following conclusions are obtained: (i) this polar 32CA reaction is topologically characterized by nine differentiated phases associated with the rupture and formation of double and single bonds, as well as the creation of non-bonding regions. This indicates that the 32CA reaction is not a concerted process;⁵ (ii) the most energetic structure along the reaction path is **S5**, which corresponds to **TS-22-m**. The energy cost demanded to reach **S5** from **S1** is 15.4 kcal mol^{−1}, mainly associated with the depopulation of the N1–N2 bonding region required to create the non-bonding

regions at the N1 and N2 nitrogens. These changes in electron density categorize this 32CA reaction as a *zw-type*;^{5,10} (iii) formation of the first N1–C4 single bond takes place at structure **S7**, at an N1–C4 distance of 1.69 Å, with an initial population of 1.17 e (see **S7** in Fig. 8), which is reached by sharing the C4 non-bonding electron density present at **S6** and some of the N1 nitrogen; (iv) the highest GEDT value along the IRC, 0.60 e, is achieved at **S8** when the first N1–C4 single bond is practically formed; (v) formation of the second N3–C5 single bond takes place at structure **S9**, at an N3–C5 distance of 1.87 Å, and with an initial population of 1.24 e (see **S9** in Fig. 8), by donation of part of the non-bonding electron density of the N3 center present at **S8** to the C5 carbon; and finally, (vi) the formation of the second N3–C5 single bond begins when the first N1–C4 single bond has reached a population of 1.69 e. This behavior characterizes the reaction mechanism of this *zw-type* 32CA reaction as a non-concerted *two-stage one-step* mechanism.⁴²

2.4. REG-IQA analysis of the activation energies in the 32CA reactions of phenyl azide **6** with supernucleophilic vinyl amines

Liu *et al.* used energy decomposition analyses^{43,44} (EDAs), such as the distortion/interaction energy¹⁷ and activation strain models,¹⁸ to analyze the chemical reactivity of phenyl azide **6**.¹⁶ It was proposed that lower distortion energies of the ethylene derivatives, resulting from more favourable FMO interactions, are responsible for the reactivity trend in the 32CA reactions of phenyl azide **6**.¹⁶ However, it is worth noting that these methods and, consequently, the interpretations that arise from it have shown to be prone to flaws due to the process-dependency of their energy components,^{45,46} which include MO interactions.

To determine the origin of the large activation energy decrease in the *zw-type* 32CA reactions of phenyl azide **6** with supernucleophilic vinyl amines, the Relative Energy Gradient⁴⁷ (REG) method was used together with the Interacting Quantum Atoms⁴⁸ (IQA) energy partitioning scheme.⁴⁹ These analyses were conducted along the most and least favourable 32CA reactions of phenyl azide **6** with supernucleophilic vinyl amine **22** and strongly electrophilic acrylonitrile **40**, respectively (see sections 7 and 8 in the ESI† for theoretical details on REG-IQA).

First, the differences between the total IQA energies of the reactant frameworks at the TSs and the first structures of the reaction paths, given in Table 4, were analysed. These values show that the phenyl azide framework is remarkably stabilized by −26.8 kcal mol^{−1} in the polar 32CA reaction involving supernucleophilic vinyl amine **22**, while it is destabilized by 8.5 kcal mol^{−1} in the non-polar reaction involving electrophilic acrylonitrile **40**. Therefore, it can be concluded that the strong stabilization of the azide framework, as a consequence of the GEDT taking place in a REDF 32CA reaction, is the main factor responsible for the decrease in activation energy.⁵⁰ In particular, a comparison of the total IQA energies at the atoms of the phenyl azide moiety in both reactions (see Table S7 in the ESI†) reveals that the N1 nitrogen and the phenyl C3' carbon

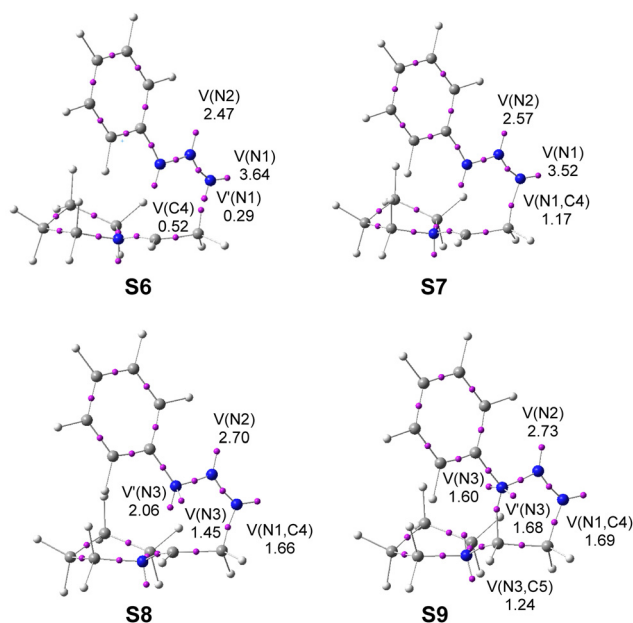
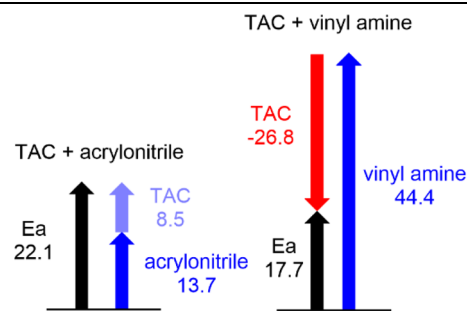


Fig. 8 ELF basin attractor positions, with the most significant valence basin populations given as the average number of electrons, e, of the **S6–S9** structures of the IRC involved in the formation of the two new N–C single bonds obtained by BET analysis at the ω B97X-D/6-311G (d,p) level in the gas phase.



Table 4 Differences between the total IQA energies, in kcal mol⁻¹, of each of the two interacting frameworks at the TSs and the first structure of the reaction paths, **S1**, for the 32CA reactions of phenyl azide **6** with supernucleophilic vinyl amine **22** and strongly electrophilic acrylonitrile **40**

	Vinyl amine 22	Azide 6	
S1-22	-289.8530	-395.8172	TAC + vinyl amine
TS-22-<i>m</i>	-289.9238	-395.7745	
ΔE	44.4	-26.8	
	Acrylonitrile 40	Azide 6	
S1-40	-170.7818	-395.7603	TAC + acrylonitrile
TS-40-<i>o</i>	-170.8036	-395.7738	
ΔE	13.7	8.5	



are the ones most stabilized in the polar process compared to the non-polar one, by 11.1 and 5.7 kcal mol⁻¹, respectively.

In order to obtain a more detailed description of the effect of this stabilization on the reaction rates, the contributions of the fully-decomposed IQA terms to the activation energies were analysed (see Table S8†). The REG-IQA analysis indicates that the rupture of the azide N1–N2 multiple bond is the factor most contributing to the barrier in the polar reaction with vinyl amine **22** (see the REG values in Table S8†), in complete agreement with the BET study given above. Instead, the rupture of the ethylene C4–C5 double bond has the greatest weight in the non-polar reaction with acrylonitrile **40**, which is in agreement with the recent REG-IQA study of the non-polar *zw-type* 32CA reaction of the simplest nitrene **3** with ethylene **5**.⁴⁹ Finally, the factor most working against the barrier in both reactions is the interaction in the region of the first N–C single bond to be formed.

The relative IQA energies of the most relevant factors do not account for the lower activation energy with vinyl amine **22**. A more profound inspection reveals that the N3 atom and the substituents play a significant role. The $E_{\text{intra}}(\text{N3})$ term is 20.1 kcal mol⁻¹ less destabilizing in the polar reaction. This is because in the polar reaction, the N3 nitrogen places the phenyl substituent completely orthogonal in order to permit the conjugation with the electrophilic azide system and an effective delocalization of the electron density received *via* the GEDT from nucleophilic ethylenes. Indeed, conjugation in the N3–C3' region is 13.1 kcal mol⁻¹ stronger in the polar reaction (see the costs of $V_{\text{xc}}(\text{N3}, \text{C3}')$ in Table S8†). In contrast, given the unlikelihood of the phenyl aromatic ring giving electron density in either FEDF or NEDF 32CA reactions due to the loss of aromaticity, the N3 nitrogen is rather bent in the non-polar reaction involving acrylonitrile **40** in order to prevent any conjugation between the azide and the aromatic ring (see the geometries of **TS-18-*m*** and **TS-15-*o*** in Fig. 4). This behavior causes an unfavorable geometric environment at the N3, which costs 34.7 kcal mol⁻¹, according to $E_{\text{intra}}(\text{N3})$.

The present REG-IQA analysis allows concluding that the large decrease in activation energies in the *zw-type* 32CA reac-

tions of phenyl azide **6** with supernucleophilic vinyl amines is a consequence of the greater stabilization of phenyl azide **6** achieved by the high GEDT in REDF 32CA reactions when this TAC acts as an electrophile, which is aided by conjugation and electrostatic effects of substitution. Thus, the low reactivity of phenyl azide **6** in both FEDF and NEDF 32CA reactions is due to the unfavorable tendency of **6** to exchange electron density probably owing to the loss of the aromatic character of the phenyl substituent. Accordingly, the only property of vinyl amines that has a decisive role in the reaction rate is their supernucleophilic character, which considerably forces the GEDT towards phenyl azide **6**, and not any distortion as previously suggested,¹⁶ which is only a geometric consequence of the density changes.

3. Conclusions

The *zw-type* 32CA reactions of phenyl azide **6** with a series of 25 ethylenes of different electrophilic and nucleophilic activation have been studied within MEDT at the ω B97X-D/6-311G(d,p) computational level in order to understand the low reactivity of this azide compared to other zwitterionic TACs. A chemical rationalization of Sustmann's "parabolic correlation" has also been established.

ELF topological analysis at the GS electronic structure of phenyl azide **6** characterizes this TAC as a zwitterionic species participating in *zw-type* 32CA reactions. Notably, the charge distribution of this TAC does not correspond to the charge distribution in the proposed 1,2-dipolar structure of azides.

Analysis of the reactivity indices of phenyl azide **6** allows characterizing this TAC as a moderate electrophile and a moderate nucleophile. Consequently, it is expected that phenyl azide **6** will have a low tendency to participate in polar 32CA reactions, a requirement demanded by *zw-type* 32CA reactions to take place easily.⁵

The study of the *zw-type* 32CA reactions of phenyl azide **6** with 18 selected ethylenes permits us to obtain some important conclusions: (i) while the 32CA reactions with electrophi-



lic ethylenes present high activation energies close to that with ethylene 5, the 32CA reactions involving the supernucleophilic vinyl amines experience a strong decrease of the activation energies, showing the preferential reactivity of phenyl azide 6 only with supernucleophilic vinyl amines; (ii) the activation energies of the low polar 32CA reactions involving strained cycloalkenes and cycloalkynes are lowered by less than 5 kcal mol⁻¹, with respect to that with ethylene 5, as a result of the loss of the ring strain that occurs along the reaction path; and (iii) while the 32CA reactions of phenyl azide 6 with electrophilic ethylenes exhibit low *ortho* regioselectivity, those involving strongly nucleophilic ethylenes are completely *meta* regioselective.

Analysis of the relative reaction rate constants k_r of 12 selected 32CA reactions, compared to those with ethylene 5, and the analysis of the reactivity indices of the corresponding ethylenes enable us to classify the *zw-type* reactions of phenyl azide 6 into four differentiated groups: (i) group A, involving supernucleophilic ethylenes, with $N \geq 4.00$ eV, and exhibiting $k_r > 10^4$; (ii) group B, comprising strained cycloalkanes and cycloalkynes, with $3.10 < N < 2.70$ eV, and displaying $k_r < 10^2$; (iii) group C, consisting of strongly electrophilic ethylenes, $\omega > 1.70$ eV, and showing $k_r \leq 10^2$; and finally, (iv) group D, encompassing moderately electrophilic ethylenes, $\omega > 1.50$ eV, and moderately nucleophilic ethylenes $N < 3.00$ eV, and displaying very low reactivity with $k_r < 2$. Although the ring strain present in cycloalkenes and cycloalkynes can accelerate the corresponding SP-32CA reaction by 10^2 times, it is only the adequate electronic nucleophilic activation of the ethylene that can accelerate the polar *zw-type* 32CA reaction by more than 10^4 times. These four groups are characterized by Sustmann's "parabolic correlation" given in Fig. 6.

The present MEDT study establishes the low reactivity of phenyl azide 6 participating in *zw-type* 32CA reactions. Phenyl azide 6 does not have "ambiphilic behavior", as recently proposed by Liu *et al.*,¹⁶ but rather a moderate electrophilic character, which demands the participation of supernucleophilic ethylenes, such as vinyl amines, to facilitate the corresponding polar *zw-type* 32CA reactions experimentally.

A representation of the GEDT at the TSs vs. the ethylenes' nucleophilic character allows demystifying the "hypothetical Sustmann's parabola graph". These 32CA reactions are not of "type II" as Sustmann proposed,¹⁴ but instead, they fall into categories of REDF for strongly nucleophilic ethylenes and FEDF for strongly electrophilic ethylenes. The present MEDT study explains the asymmetry of the "Sustmann's parabola" in Fig. 1, revealing that only the upper-left branch of the graph exhibits significant acceleration and complete *meta* regioselectivity, which is synthetically valuable.

Finally, REG-IQA analysis of the activation energy of the 32CA reaction of phenyl azide 6 with vinyl amine 22 indicates that the greater stabilization of the azide framework facilitated by the GEDT when it acts as an electrophile toward supernucleophilic vinyl amines is the main factor driving the large acceleration, in which conjugation with the phenyl substituent plays a relevant role.

Author contributions

L.R.D. data curation, formal analysis, funding acquisition, investigation, supervision, writing – original draft and writing – review & editing. M.R.G. data curation, investigation, writing – original draft and writing – review & editing. P.P. data curation, investigation, supervision, writing – original draft and writing – review & editing.

Conflicts of interest

The authors declare no conflict of interest.

Acknowledgements

This work has been supported by the Ministry of Science and Innovation (MICINN) of the Spanish Government, project PID2019-110776GB-I00 (AEI/FEDER, UE), and by FONDECYT – Chile through Project No. 1221383. L. R. D. also acknowledges Cooperación Internacional (Fondecyt No. 1221383) for continuous support.

References

- 1 W. Carruthers, in *Some Modern Methods of Organic Synthesis*, Cambridge University Press, Cambridge, 2nd edn, 1978.
- 2 A. Padwa, in *1,3-Dipolar Cycloaddition Chemistry*, Wiley-Interscience, New York, NY, USA, 1984; Vol. 1 and 2.
- 3 W. Carruthers, in *Cycloaddition Reactions in Organic Synthesis*, Pergamon, Oxford, 1990.
- 4 A. Padwa and W. H. Pearson, in *Synthetic Applications of 1,3-Dipolar Cycloaddition Chemistry Toward Heterocycles and Natural Products*, John Wiley & Sons, Inc., New York, NY, USA, 2002, Vol. 59.
- 5 M. Ríos-Gutiérrez and L. R. Domingo, Unravelling the Mysteries of the [3 + 2] Cycloaddition Reactions, *Eur. J. Org. Chem.*, 2019, 267–282.
- 6 R. Huisgen, Kinetics and Mechanism of 1,3-Dipolar Cycloadditions, *Angew. Chem., Int. Ed. Engl.*, 1963, 2, 633–645.
- 7 R. A. Firestone, Mechanism of 1,3-dipolar cycloadditions, *J. Org. Chem.*, 1968, 33, 2285–2290.
- 8 L. R. Domingo, Molecular Electron Density Theory: A Modern View of Reactivity in Organic Chemistry, *Molecules*, 2016, 21, 1319.
- 9 M. Ríos-Gutiérrez, L. R. Domingo and R. Jasiński, Unveiling the High Reactivity of Experimental Pseudodiradical Azomethine Ylides within Molecular Electron Density Theory, *Phys. Chem. Chem. Phys.*, 2023, 25, 314–325.
- 10 L. R. Domingo, M. Ríos-Gutiérrez and P. Pérez, A Molecular Electron Density Theory Study of the Reactivity and Selectivities in [3 + 2] Cycloaddition Reactions of C,



- N-Dialkyl Nitrones with Ethylene Derivatives, *J. Org. Chem.*, 2018, **83**, 2182–2197.
- 11 K. Fukui, in *Molecular Orbitals in Chemistry, Physics, and Biology*, New York, 1964.
 - 12 R. S. Mulliken, Spectroscopy, molecular orbitals and chemical bonding, *Science*, 1967, **157**, 13–24.
 - 13 E. R. Scerri, Have Orbitals Really Been Observed?, *J. Chem. Educ.*, 2000, **77**, 1492–1494.
 - 14 R. Sustmann and H. Trill, Substituent Effects in 1,3-Dipolar Cycloadditions of Phenyl Azide, *Angew. Chem., Int. Ed. Engl.*, 1972, **9**, 838–840.
 - 15 R. Sustmann and R. Schubert, Substituent Effects in Diels-Alder Additions, *Angew. Chem., Int. Ed. Engl.*, 1972, **9**, 840.
 - 16 P.-P. Chen, P. Ma, X. He, D. Svatunek, F. Liu and K. N. Houk, Computational Exploration of Ambiphilic Reactivity of Azides and Sustmann's Paradigmatic Parabola, *J. Org. Chem.*, 2021, **86**, 5792–5804.
 - 17 D. H. Ess and K. N. Houk, Theory of 1,3-Dipolar Cycloadditions: Distortion/Interaction and Frontier Molecular Orbital Models, *J. Am. Chem. Soc.*, 2008, **130**, 10187–10198.
 - 18 F. M. Bickelhaupt, Understanding reactivity with Kohn-Sham molecular orbital theory: E2–SN2 mechanistic spectrum and other concepts, *J. Comput. Chem.*, 1999, **20**, 114–128.
 - 19 L. R. Domingo and N. Acharjee, Unravelling the strain-promoted [3 + 2] cycloaddition reactions of phenyl azide with cycloalkynes from the molecular electron density theory perspective, *New J. Chem.*, 2020, **44**, 13633–13643.
 - 20 F. Schoenebeck, D. H. Ess, G. O. Jones and K. N. Houk, Reactivity and Regioselectivity in 1,3-Dipolar Cycloadditions of Azides to Strained Alkynes and Alkenes: A Computational Study, *J. Am. Chem. Soc.*, 2009, **131**, 8121–8133.
 - 21 L. R. Domingo, a new C-C bond formation model based on the quantum chemical topology of electron density, *RSC Adv.*, 2014, **4**, 32415–32428.
 - 22 L. R. Domingo, K. Kula and M. Ríos-Gutiérrez, Unveiling the Reactivity of Cyclic Azomethine Ylides in [3 + 2] Cycloaddition Reactions within the Molecular Electron Density Theory, *Eur. J. Org. Chem.*, 2020, 5938–5948.
 - 23 L. R. Domingo and M. Ríos-Gutiérrez, A Useful Classification of Organic Reactions Bases on the Flux of the Electron Density, *Sci. Radiol.*, 2023, **2**, 1.
 - 24 R. Huisgen, 1,3-Dipolar Cycloadditions. Past and Future, *Angew. Chem., Int. Ed. Engl.*, 1963, **2**, 565–598.
 - 25 H. B. El Ayouchia, B. Lahoucine, H. Anane, M. Ríos-Gutiérrez, L. R. Domingo and S.-E. Stiriba, Experimental and Theoretical MEDT Study of the Thermal [3 + 2] Cycloaddition Reactions of Aryl Azides with Alkyne Derivatives, *ChemistrySelect*, 2018, **3**, 1215–1223.
 - 26 A. D. Becke and K. E. Edgecombe, A simple measure of electron localization in atomic and molecular systems, *J. Chem. Phys.*, 1990, **92**, 5397–5403.
 - 27 B. Silvi and A. Savin, A. Classification of chemical bonds based on topological analysis of electron localization functions, *Sci. Rad.*, 1994, **371**, 683–686.
 - 28 A. E. Reed, R. B. Weinstock and F. Weinhold, Natural population analysis, *J. Chem. Phys.*, 1985, **83**, 735–746.
 - 29 E. Reed, L. A. Curtiss and F. Weinhold, Intermolecular interactions from a natural bond orbital, donor-acceptor viewpoint, *Chem. Rev.*, 1988, **88**, 899–926.
 - 30 R. G. Parr and W. Yang, *Density Functional Theory of Atoms and Molecules*, Oxford University Press, New York, 1989.
 - 31 L. R. Domingo, M. Ríos-Gutiérrez and P. Pérez, Applications of the conceptual density functional indices to organic chemistry reactivity, *Molecules*, 2016, **21**, 748.
 - 32 L. R. Domingo and M. Ríos-Gutiérrez, Application of Reactivity Indices in the Study of Polar Diels-Alder Reactions, in *Conceptual Density Functional Theory: Towards a New Chemical Reactivity Theory*, ed. S. Liu, Wiley-VCH GmbH, 2022, Vol. 2, pp. 481–502.
 - 33 R. G. Parr, L. v. Szentpaly and S. Liu, Electrophilicity index, *J. Am. Chem. Soc.*, 1999, **121**, 1922–1924.
 - 34 L. R. Domingo, E. Chamorro and P. Pérez, Understanding the reactivity of captodative ethylenes in polar cycloaddition reactions, A theoretical study, *J. Org. Chem.*, 2008, **73**, 4615–4624.
 - 35 T. Kondo, H. Ono, N. Satake, T. Mitsudo and Y. Watanabe, Nucleophilic and Electrophilic Allylation Reactions. Synthesis, Structure, and Ambiphilic Reactivity of (η^3 -Allyl) ruthenium(II) Complexes, *Organometallics*, 1995, **14**, 1945–1953.
 - 36 C. Cardenas, N. Rabi, P. W. Ayers, C. Morell, P. Jaramillo and P. Fuentealba, Chemical Reactivity Descriptors for Ambiphilic Reagents: Dual Descriptor, Local, and Electrostatic Potential, *J. Phys. Chem. A*, 2009, **113**, 8660–8667.
 - 37 R. G. Parr and R. G. Pearson, Absolute hardness: Companion parameter to absolute electronegativity, *J. Am. Chem. Soc.*, 1983, **105**, 7512–7516.
 - 38 L. R. Domingo, M. Ríos-Gutiérrez and P. Pérez, A Molecular Electron Density Theory Study of the Reactivity of Tetrazines in Aza-Diels-Alder Reactions, *RSC Adv.*, 2020, **10**, 15394–15405.
 - 39 L. R. Domingo, M. J. Aurell, P. Pérez and R. Contreras, Quantitative characterization of the global electrophilicity power of common diene/dienophile pairs in Diels-Alder reactions, *Tetrahedron*, 2002, **58**, 4417–4423.
 - 40 M. G. Evans, Some applications of the transition state method to the calculation of reaction velocities, especially in solution, *Trans. Faraday Soc.*, 1935, **31**, 875–894.
 - 41 K. Krokidis, S. Noury and B. Silvi, Characterization of Elementary Chemical Processes by Catastrophe Theory, *J. Phys. Chem. A*, 1997, **101**, 7277–7282.
 - 42 L. R. Domingo, J. A. Sáez, R. J. Zaragoza and M. Arnó, Understanding the Participation of Quadricyclane as Nucleophile in Polar $[2\sigma + 2\sigma + 2\pi]$ Cycloadditions toward Electrophilic π Molecules, *J. Org. Chem.*, 2008, **73**, 8791–8799.
 - 43 K. Kitaura and K. Morokuma, A new energy decomposition scheme for molecular interactions within the Hartree-Fock approximation, *Int. J. Quantum Chem.*, 1976, **10**, 325–340.



- 44 K. Morokuma and K. Kitaura, in *Chemical Applications of Atomic and Molecular Electrostatic Potentials*, Plenum, New York, 1981, pp. 215–242.
- 45 D. M. Andrada and C. Foroutan-Nejad, Energy components in energy decomposition analysis (EDA) are path functions; why does it matter?, *Phys. Chem. Chem. Phys.*, 2020, **22**, 22459–22464.
- 46 J. Poater, D. M. Andrada, M. Solà and C. Foroutan-Nejad, Path-dependency of energy decomposition analysis & the elusive nature of bonding, *Phys. Chem. Chem. Phys.*, 2022, **24**, 2344–2348.
- 47 J. C. R. Thacker and P. L. A. Popelier, The ANANKE relative energy gradient (REG) method to automate IQA analysis over configurational change, *Theor. Chem. Acc.*, 2017, **136**, 86.
- 48 M. A. Blanco, A. Martín Pendás and E. Francisco, Interacting Quantum Atoms: A Correlated Energy Decomposition Scheme Based on the Quantum Theory of Atoms in Molecules, *J. Chem. Theory Comput.*, 2005, **1**, 1096–1109.
- 49 M. Ríos-Gutiérrez, F. Falcioni, L. R. Domingo and P. L. A. Popelier, A Combined BET and IQA-REG Study of the Activation Energy of non-polar zw-type [3 + 2] Cycloaddition Reactions, *Phys. Chem. Chem. Phys.*, 2023, **25**, 10853–10865.
- 50 L. R. Domingo, M. Ríos-Gutiérrez and P. Pérez, how does the global electron density transfer diminish activation energies in polar cycloaddition reactions? A Molecular Electron Density Theory study, *Tetrahedron*, 2017, **73**, 1718–1724.

